

## **Reference material**

### *Reference books:*

Y.C. Fung, "Foundations of Solid Mechanics", Prentice Hall

R. Hill, "The mathematical theory of plasticity", Oxford University Press, Oxford.

J. Lubliner, "Plasticity theory", Mcmillan Publishing Company, New York.

L. Kachanov, "Foundations of the theory of plasticity", North-Holland Publishing Company, Amsterdam.

W. Johnson, P. Mellor, "Plasticity for mechanical engineers", D. Van Nostrand Company, Ltd, London.

A. Mendelsohn, "Plasticity: Theory and Application", Mcmillan Publishing Company, New York.

## 1. Experimental observations of plastic deformation

In addition to elastic and visco-elastic deformation behavior, materials can undergo plastic deformation. The main characteristic of plastic deformation is that it is irreversible. Plastic deformation can be virtually instantaneous or time-dependent depending on the conditions under which deformation takes place. The main controlling variables are temperature and deformation rate. The wide range of possible material behavior during deformation is best illustrated in the following deformation map from Frost and Ashby:

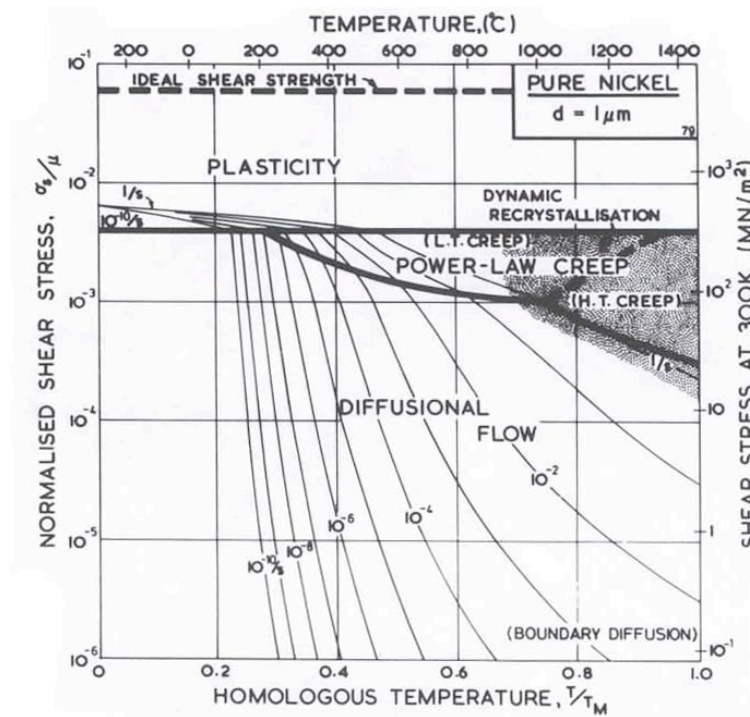


Fig. 1.1. Typical deformation mechanism map for pure, work hardened Ni with 1  $\mu\text{m}$  grain size

We will be mostly concerned with instantaneous or time-independent, permanent deformation or plastic deformation for short. Figure 1.2 is a schematic load-extension diagram when a specimen is plastically deformed in a tensile test. *Initial yield* occurs at a with departure from linearity. Range oa is called the *elastic region*. Only for some very high-strength metals is it possible to have nonlinear elastic behavior prior to internal yield. If the specimen is deformed beyond a to b and then the load is reduced to zero, the permanent deformation oc remains. The slope of cb is to a very good approximation the same as that of oa, i.e., proportional to Young's modulus  $E$ . The point of maximum load

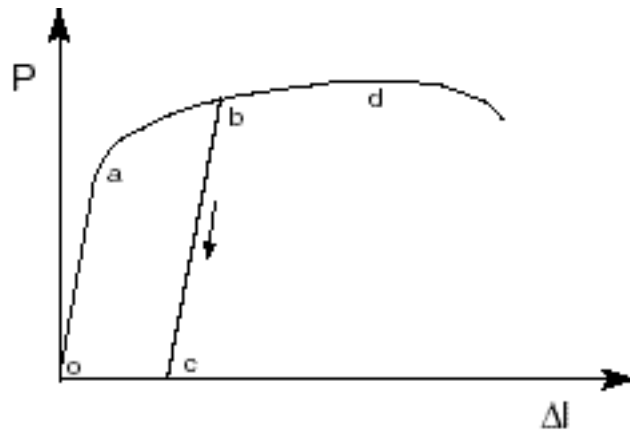


Fig. 1.2. is a typical load-extension diagram

is *d*. At or near this point localized necking begins and the specimen no longer deforms uniformly. At some point past *d* the specimen fractures. Necking is a material-geometric instability in which strain hardening of the material is insufficient to compensate for a local reduction in cross-sectional area. If one could obtain tensile data past the necking point, one would find that the true stress,  $\sigma = P / A$ , increases monotonically until failure starts. Typically, the initial yield strain is between 0.1 and 1% while the strain at necking is 10 to 40 times larger. There is virtually no permanent change in volume after the specimen has been deformed. Furthermore, the force-elongation curve is essentially unchanged when the specimen has hydrostatic pressure superimposed on it. Hydrostatic pressure alone induces almost no permanent deformation.

Plastic deformation of typical structural materials can be considered rate-independent at room temperature and at normal strain-rates. For strain rates in the range of  $10^{-6}$  / sec. to 10 / sec, the behavior is relatively insensitive to the strain-rate at which the test is conducted. If the temperature is a significant fraction of the melting temperature (in Kelvin), however, the strain-rate sensitivity becomes marked. Tin or lead are examples where even at room temperature rate effects play a role. Figure 1.3 shows the result of tests conducted at constant strain-rate ( $\dot{\epsilon}_1 < \dot{\epsilon}_2 < \dot{\epsilon}_3$ ). The strain-rate dependence increases with increasing temperature. Rate effects are also more important in BCC than FCC materials. In what follows, we will assume that the temperature is low enough that *strain-rate effects can be neglected*, and we will consider *time-independent plasticity*. Typically, this means the temperature is below about 0.4 times the melting temperature on an

absolute temperature scale (see deformation mechanism map in Figure 1.1). Above 0.4 times the melting temperature, creep becomes important (see Figure 1.3).

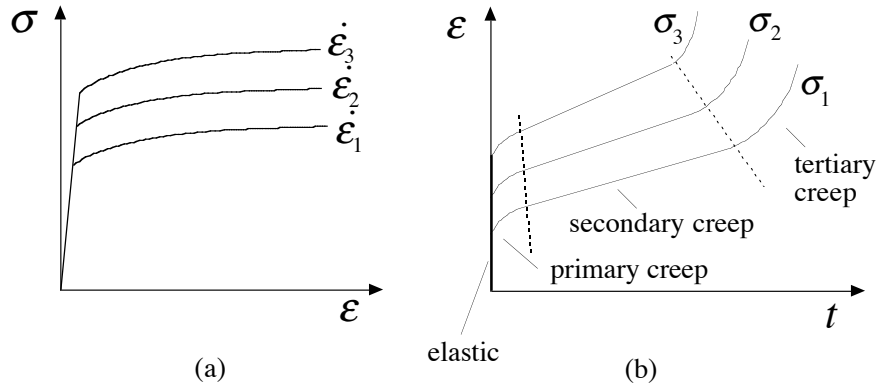


Fig 1.3. (a) Tests conducted at different constant strain rates; (b) tests conducted at different constant stress  $\sigma_3 > \sigma_2 > \sigma_1$  (creep tests).

## 2. Foundations of plasticity

In order to determine the stresses and strains in a body subjected to external forces, we can use the equations discussed in the previous section. In addition to these equations (i.e., definitions of stress and strain, compatibility and equilibrium equations, boundary conditions), we also need equations linking stresses and strains. These equations are the constitutive equations of the material under consideration and they are obviously material dependent. In the following sections, we will describe the plastic response of a material in the presence of a stress field.

### 2.1. Characterization of deformation under uniaxial stress

Consider a tensile specimen in a uniaxial stress state  $\sigma$ . Figure 2.1 is a schematic representation of the stress-strain curve. Let  $\sigma_y^o$  be the *initial* yield stress in tension and  $\sigma_y$  be the *current* yield stress in tension, i.e.,  $\sigma_y = \max(\sigma)$ . From observation, we know that at a given stress level  $\sigma$ , the total strain  $\varepsilon$  comprises both elastic strain  $\varepsilon^e$  and plastic strain  $\varepsilon^P$  (See Fig. 2.1):

$$\varepsilon = \varepsilon^e + \varepsilon^P, \quad (2.1)$$

where the elastic strain is given by  $\varepsilon^e = \sigma / E$ . We then define the tangent modulus as follows:

$$E_t = \frac{d\sigma}{d\varepsilon} \text{ or } \dot{\sigma} = E_t \dot{\varepsilon}, \quad (2.2)$$

where  $E_t$  is of course a function of the stress  $\sigma$ . Thus, we find the following expression for the plastic strain rate as a function of the tangent modulus

$$\dot{\varepsilon}^P = \dot{\varepsilon} - \dot{\varepsilon}^e = \left( \frac{1}{E_t} - \frac{1}{E} \right) \dot{\sigma}. \quad (2.3)$$

We define the secant modulus as follows:

$$E_s = \frac{\sigma}{\varepsilon} \quad (2.4)$$

where  $E_s$  is again a function of the stress  $\sigma$ . The total plastic strain can then be written as a function of the secant modulus

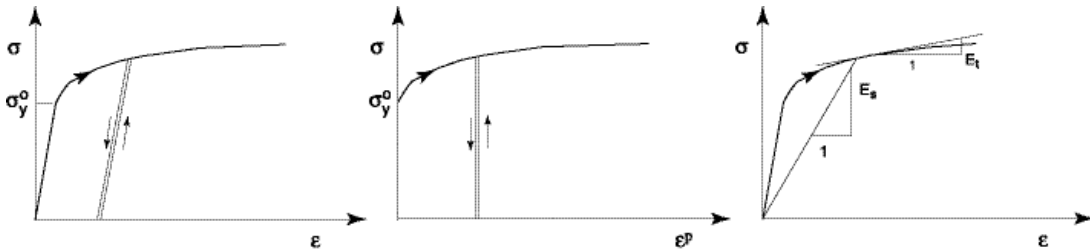


Fig. 2.1. Definition of secant and tangent moduli

$$\varepsilon^p = \varepsilon - \varepsilon^e = \left( \frac{1}{E_s} - \frac{1}{E} \right) \sigma. \quad (2.5)$$

In the next few paragraphs, we present a number of simple mathematical models to describe experimental uniaxial stress-strain curves of metal alloys. These mathematical representations are important for two reasons. First, these “laws” incorporate parameters that can be used to compare the resistance of materials to plastic deformation (this is a “Material Science” point of view). Second, analytical formulae are necessary in order to allow analytical or closed-form analyses of mechanical problems. The following models are sometimes used to describe uniaxial deformation behavior:

*1. The Ramberg-Osgood stress strain curve*

The virgin curve of a workhardening solid is frequently approximated by the Ramberg-Osgood formula

$$\varepsilon = \frac{\sigma}{E} + \alpha \frac{\sigma_R}{E} \left( \frac{\sigma}{\sigma_R} \right)^m, \quad (2.6)$$

where  $\alpha$  and  $m$  are dimensionless constants, and  $\sigma_R$  is a reference stress. If  $m$  is very large, then  $\varepsilon^p$  remains small until  $\sigma$  approaches  $\sigma_R$ , and increases rapidly when  $\sigma$  exceeds  $\sigma_R$ , so that  $\sigma_R$  may be regarded as an approximate yield stress. In the limit when  $m$  becomes infinite, the plastic strain is zero when  $\sigma < \sigma_R$ , and indeterminate when  $\sigma = \sigma_R$ , while  $\sigma > \sigma_R$  would produce an infinite plastic strain and is therefore impossible. This limiting case accordingly describes an elastic perfectly plastic solid with yield stress  $\sigma_R$ . The Ramberg-Osgood representation has the advantage not to be piecewise, i.e., it has a continuous derivative. It agrees with Hooke’s law only for  $\sigma \rightarrow 0$  and should be used for

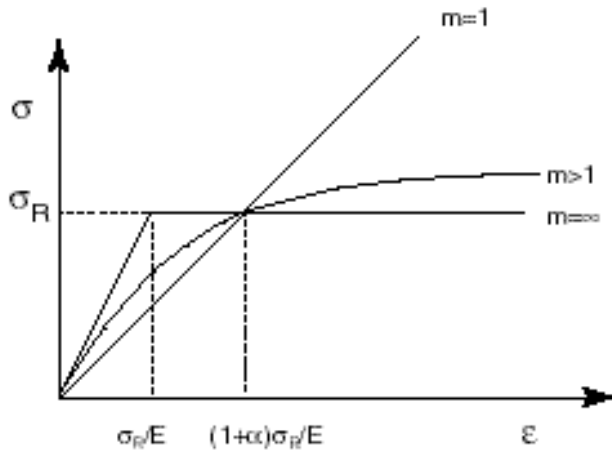


Fig. 2.2. Schematic representation of the Ramberg-Osgood formula

problems involving a significant amount of plastic straining (i.e.,  $\epsilon^p \gg \sigma_R/E$ ). Note that expressing the stress as a function of strain requires solving a non-linear equation.

### 2. Power hardening law

If the deformation is sufficiently large for the elastic strain to be neglected, then Eq. (2.6) can be solved for  $\sigma$  in terms of  $\epsilon$ , resulting in the following expression:

$$\sigma = C\epsilon^n, \quad (2.7)$$

where  $n=1/m$  is often called the work-hardening exponent. Note that the stress-strain curve represented by the power law equation has an infinite slope at the origin. In order to get around this problem one sometimes uses the piecewise power law.

### 3. Piecewise power hardening law

The piecewise power hardening law is given by:

$$\sigma = \begin{cases} E\epsilon & \epsilon \leq \frac{\sigma_y^o}{E} \\ \sigma_y^o \left[ \frac{E\epsilon}{\sigma_y^o} \right]^n & \epsilon \geq \frac{\sigma_y^o}{E} \end{cases} \quad (2.8)$$

A graphical representation of the piecewise power hardening law is shown in Fig. 2.3.

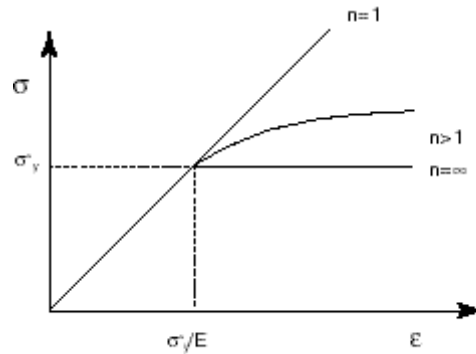


Fig. 2.3. Graphical representation of the piecewise power hardening law

### 4. Elastic-perfectly plastic

In the limit when  $m$  becomes infinite in Eq. (2.6) or  $n$  becomes zero in Eq. (2.8), we have a piecewise linear stress-strain curve representing an elastic-perfectly plastic material. This is a material that has a normal elastic range, but does not show any work hardening upon yielding. In a further simplification, we can neglect the elastic strains and we obtain the stress-strain curve of a rigid-perfectly plastic material (See Fig. 2.4).

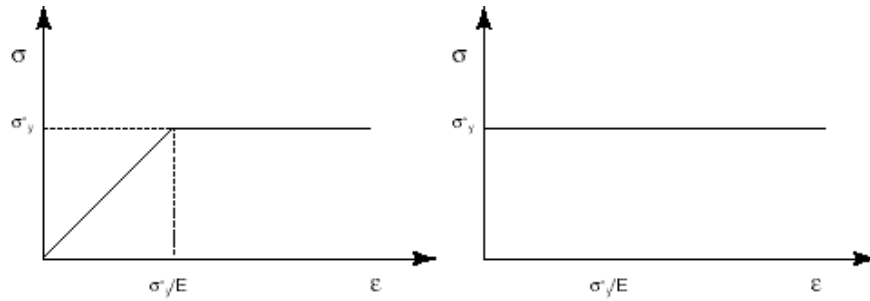


Fig. 2.4. Stress-strain curves for elastic-perfectly plastic and rigid-perfectly plastic materials, respectively.

## 2.2. Deformation behavior in multiaxial stress-strain states

It is relatively straightforward to characterize the deformation behavior of a material in a simple uniaxial stress-state. It is important, however, to know the behavior of a material in a complex multiaxial stress state as well. In particular, we need to know when the deformation behavior changes from elastic to plastic. The aim of this section is to build up constitutive theories of plasticity. The other ingredients of a solid mechanics theory are unchanged: definition of stress (statics), definition of strain (kinematics), compatibility relationships, equilibrium equations, and the boundary conditions belonging to each specific problems. A general constitutive theory aims at relating all the components of the stress tensor to all the components of the strain tensor through a function  $F$ , which may depend on several variables:

$$\boldsymbol{\varepsilon} = F(\boldsymbol{\sigma}, A_1, \dots, A_n)$$

where the  $A_i$ 's are all possible variables that affect the mechanical response of a material (elastic moduli, indicators of the stress and strain histories, temperature, strain rate, the yield stresses for the different slip systems, the hardening coefficient for all slip systems, parameters related to recrystallization, crystallographic orientation distribution functions, dislocation substructure cell sizes,...).

In the macroscopic theory of plasticity presented in this section, only macroscopic variables are considered: elastic moduli, indicators of the stress and strain histories, current stress and strain state, temperature, strain rate, macroscopic yield stress (or yield stresses for anisotropic theories), macroscopic hardening coefficient (or coefficients for anisotropic theories). Physically, stresses and strains in such a theory have a meaning at a level where non-uniformity in the microstructure (inclusions, second phases, grain



boundaries, grain interactions, texture effects, ...) are averaged. For typical metals, a representative volume element, i.e. the smallest volume element, which contains all information about the material<sup>1</sup>, must have a large number of grains (>100), depending on the texture. Representative volume elements for polycrystals will range from smaller than  $10 \times 10 \times 10 \text{ } \mu\text{m}^3$  in fine-grained metals with sharp textures (a "sharp texture" means that almost all grains are oriented identically and thus a smaller number of grains is necessary to get good averaging) to larger than  $1 \times 1 \times 1 \text{ mm}^3$  for large-grained materials.

Here we will discuss the *incremental theory of plasticity*. Plasticity is intrinsically path-dependent and the incremental theory accounts for loading history. The natural way to build a mathematical theory involving history effects is to relate stress increments to strain increments and not the total stress to the total strain. We will show the general features of the incremental theory of plasticity and then study to the simplest theory,  $J_2$ -incremental theory, which involves the variable  $J_2$ , a criterion on whether plastic loading or elastic loading or unloading occurs, and the current state of stress.

In the most general case, the *initial transition* from elastic to plastic deformation of an initially isotropic material depends on the complete state of stress at the point under consideration. In order to make it easier to describe this, we introduce a six-dimensional Cartesian stress (or strain) space, where every point represents a particular stress (strain) state determined by the six independent element of the stress (or strain) tensor. If we use the principal stresses ( $\sigma_1, \sigma_2, \sigma_3$ ) as coordinates, we speak of the *Haigh-Westergaard* stress space. A *stress-history* is then defined as a locus of stress-states in stress space. A *radial loading path* or *radial stress history* is a straight line in stress space passing through the origin. This is also called a *proportional loading path*.

The region in stress space where the material behaves elastically is separated from the region where the material deforms plastically by a surface. This surface is called the yield surface of the material and can be represented mathematically by

$$F(\sigma_{ij}) = 0. \tag{2.9}$$

Equation (2.9) represents a hypersurface in the six-dimensional stress space and any point on this surface represents a point where yielding can begin.

---

<sup>1</sup> this also means that if the size of the representative volume element is doubled, the same relationship between the stresses and strains will be found.

If the stress is on the current yield surface and if the stress increment is such that the stress leaves the yield surface then *elastic unloading*, unloading for short, is said to have occurred. If a plastic strain increment occurs due to the stress increment "pushing into" the yield surface then *loading* occurs. If the stress increment is *tangent* to the yield surface then the plastic strain increment is zero and *neutral loading* is said to have occurred, as will be discussed in more detail below.

We mentioned in the introduction that to a very good approximation plastic deformation does not change the volume of the material and that the hydrostatic pressure

$$p = -\frac{1}{3}\sigma_{kk} \quad (2.10)$$

has no effect on the plastic strains. Thus, the plastic strains,  $\epsilon_{ij}^p$ , depend only on the history of the stress deviator

$$s_{ij} = \sigma_{ij} - \frac{1}{3}\sigma_{kk}\delta_{ij}. \quad (2.11)$$

Since plastic deformation conserves volume, we also have

$$\epsilon_{kk}^p = 0. \quad (2.12)$$

Let's now consider an initially isotropic material, at least as far as plastic properties are concerned. Rotating the coordinate axes should not affect the yield behavior and we can choose the principal axes for the coordinates. For an isotropic material the order of the stresses is unimportant. The expression for the yield surface, Eq. (2.9), can then be written as

$$F_1(\sigma_1, \sigma_2, \sigma_3) = 0. \quad (2.13)$$

Since the hydrostatic pressure does not influence yielding, only the deviatoric components of the stress tensor enter into the equation for the yield surface and we can write

$$F_2(s_1, s_2, s_3) = 0, \quad (2.14)$$

where  $s_1$ ,  $s_2$ , and  $s_3$  are the principal stresses of the stress deviator. Since there is a one to one correspondence between principal stresses and stress invariants

$$\begin{aligned} J_1 &= s_1 + s_2 + s_3, \\ J_2 &= -(s_1s_2 + s_2s_3 + s_3s_1), \\ J_3 &= s_1s_2s_3, \end{aligned} \quad (2.15)$$

and keeping in mind that the first invariant of the deviator is zero, we can replace Eq. (2.14) with

$$f(J_2, J_3) = C, \quad (2.16)$$

where C is a constant. Note that invariants used in Eq. (2.16), are the *invariants of the stress deviator* defined in Eq. (2.11), not those of the stress tensor  $[\sigma_{ij}]$ . With the additional assumption that both  $\sigma_{ij}$  and  $-\sigma_{ij}$  are on the yield surface, we find

$$f(J_2, J_3^2) = C. \quad (2.17)$$

**Exercise:** Show all of the following equalities:

$$J_2 = \frac{1}{2} s_{ij} s_{ij} = \frac{1}{2} (s_1^2 + s_2^2 + s_3^2) = \frac{1}{3} (\sigma_1^2 + \sigma_2^2 + \sigma_3^2 - \sigma_1 \sigma_2 - \sigma_2 \sigma_3 - \sigma_3 \sigma_1),$$

$$J_3 = \frac{1}{3} s_{ij} s_{jk} s_{ik} = \frac{1}{3} (s_1^3 + s_2^3 + s_3^3) = s_1 s_2 s_3.$$

### Shape of yield surfaces for isotropic materials

Consider a line L in the Haigh-Westergaard space that has equal angles with each of the coordinate axes (see Fig. 2.7). For every point on this line, the stress state is one for which:

$$\sigma_1 = \sigma_2 = \sigma_3. \quad (2.19)$$

Every point on this line corresponds to a hydrostatic stress state. The plane perpendicular to this line and passing through the origin is called the  $\pi$ -plane and has equation

$$\sigma_1 + \sigma_2 + \sigma_3 = 0. \quad (2.20)$$

Every point in the  $\pi$ -plane corresponds to a deviatoric stress state. Now consider an

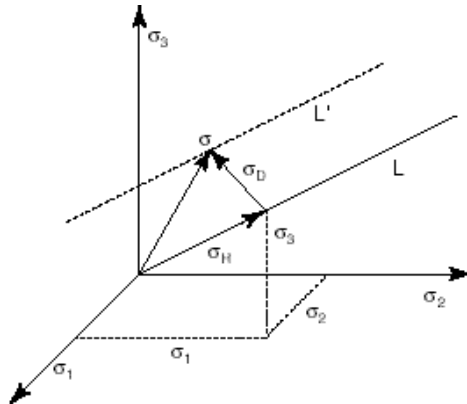


Fig. 2.7. Hydrostatic and deviatoric components in stress space.

arbitrary stress state  $\sigma$  represented by a vector in Haigh-Westergaard space. This vector can always be decomposed in a vector lying along L (the hydrostatic component) and one parallel to the  $\pi$ -plane (the deviatoric component). Clearly, any stress state on a line L' through  $\sigma$  and parallel to L has the same deviatoric component as  $\sigma$  and will differ only in the hydrostatic component. Since yielding is determined by the deviatoric component only, it follows that if one of the points on L' lies on the yield surface, they must all lie on the yield surface. The yield surface is therefore composed of lines parallel to L', or in other words, it is a *cylinder* with generators parallel to L. The only assumption we have made to come to this conclusion is that plastic deformation is independent of the hydrostatic stress.

*Examples of initial yield surfaces*

We now look in more detail at some commonly used yield surfaces.

**1. The Von Mises yield criterion**

According to the Von Mises criterion, the yield surface depends only on  $J_2$ , and is given by the following equation:

$$J_2 = C, \tag{2.21}$$

where  $C$  is a constant to be determined from the uniaxial deformation behavior. In simple tension,  $J_2$  takes on a simple form:

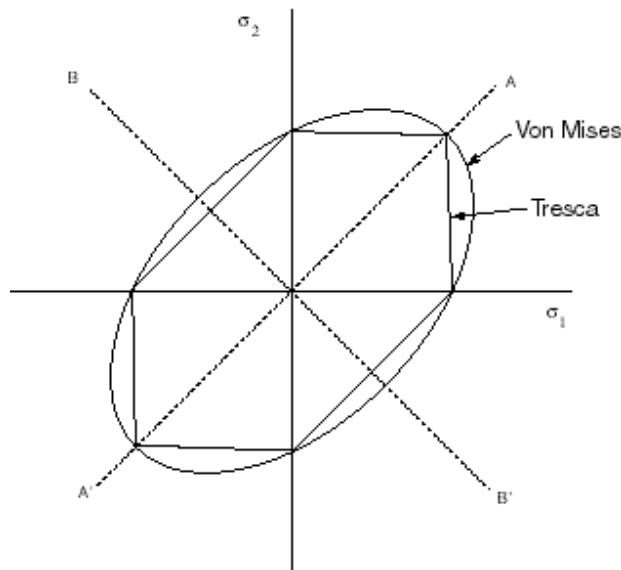


Fig. 2.8. The Tresca and Von Mises yield criteria.

$$J_2 = \frac{1}{3}\sigma^2 = \frac{1}{3}(\sigma_y^o)^2,$$

where  $\sigma_y^o$  is the initial yield stress. The Von Mises yield criterion then becomes:

$$J_2 = \frac{1}{3}(\sigma_y^o)^2 \quad (2.22)$$

or

$$(\sigma_1 - \sigma_2)^2 + (\sigma_2 - \sigma_3)^2 + (\sigma_3 - \sigma_1)^2 = 2(\sigma_y^o)^2 \quad (2.23)$$

The Von Mises criterion results in an ellipse in the  $(\sigma_1, \sigma_2)$  plane and a schematic depiction is shown in Fig. 2.8.

## 2. The Tresca yield criterion

The Tresca yield criterion is probably the oldest criterion for plastic deformation, first proposed by Tresca in 1864. According to the Tresca criterion, yield occurs if the maximum shear stress reaches a critical value. This is so when

$$\sigma_1 - \sigma_3 = 2\tau_y = \sigma_y^o, \quad (2.24)$$

where  $\tau_y$  is the yield stress in pure shear and it is assumed that  $\sigma_1 > \sigma_2 > \sigma_3$ . The Tresca criterion can be written in the form

$$4J_2^3 - 27J_3^2 - 36\tau_y^2 J_2^2 + 96\tau_y^4 J_2 - 64\tau_y^6 = 0. \quad (2.25)$$

This form of the criterion has absolutely no practical interest except to show that the Tresca criterion fits within the logical framework we have built up thus far. Figure 2.8 shows the Tresca yield criterion in the  $(\sigma_1, \sigma_2)$  plane.

It can be shown that if the yield locus is assumed to be convex and one circumscribes the Von Mises circle in the  $\pi$ -plane by a regular hexagon, then all possible yield loci must lie between the two regular hexagons inscribed in, and circumscribing the Von Mises circle. Note that the inner hexagon corresponds to the Tresca criterion. Later on, we will show that the yield surface must indeed be convex and these hexagons are real bounds to the actual yield surface. If the Von Mises criterion is taken as a reference, then the maximum deviation of any admissible yield surface is approximately 15.5%.

### 2.3. Incremental or flow theories of plasticity

As mentioned in the previous section, plasticity is a stress-history dependent phenomenon and it is necessary analyze plasticity problems with an incremental approach to take the stress history into account. Before discussing the incremental or flow theory of plasticity, we need to make a few observations on the yield surface of a stable or work hardening solid.

#### 2.3.1. Drucker's postulates

Drucker defined a stable material as a material that always dissipates energy under any closed cycle of stress. It is possible to derive mathematical equations to describe this type of behavior, but that is outside the scope of this course. We do note, however, that for stable materials

$$\dot{\epsilon}_{ij}^p \dot{\sigma}_{ij} \geq 0 ,$$

for any plastic strain increment. This inequality has some interesting consequences regarding the plastic properties of a stable material:

- 1) If the yield surface is smooth at  $\sigma_{ij}^o$ , then  $\dot{\epsilon}_{ij}^p$  is perpendicular to the yield surface.
- 2) If there is a corner at  $\sigma_{ij}^o$ , then  $\dot{\epsilon}_{ij}^p$  lies in the forward cone of normals.
- 3) The yield surface is convex.

These properties are important in the formulation of any incremental plasticity theory.

#### 2.3.2. Incremental or flow theories for materials with smooth yield surfaces

Since for plastic deformation, the stress in the final state depends on the path of deformation, the equations describing plastic strain cannot in principle be finite relations connecting the components of stress and strain. They must be non-integrable differential

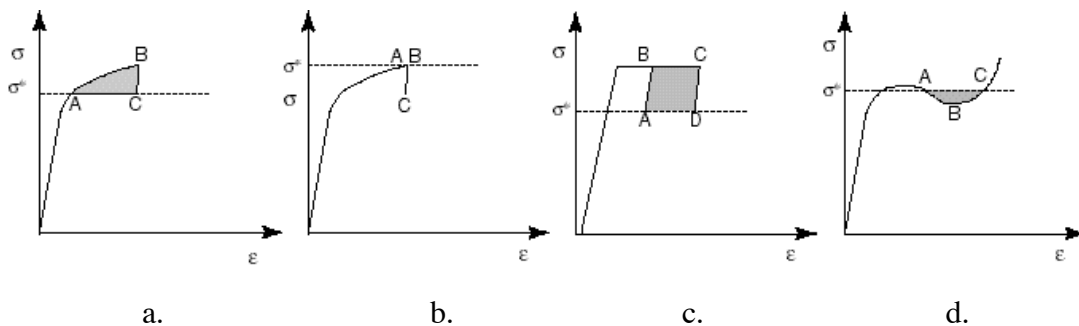


Fig. 2.13. Stress-strain curves for various materials with closed strain cycles.

relations. In this section we will discuss theories that relate the plastic strain increment to the deviatoric stress state in a solid. Unlike deformation theories, these so-called incremental or flow theories do take the stress history of a solid into account. The theory is based on the following three postulates:

- (1) There exists a *yield surface*, which in general depends on the entire previous stress history. The yield surface is taken to be smooth without corners.
- (2) The material is *stable*. This implies that the plastic strain increment is parallel to the outward normal on the yield surface.
- (3) The relationship between strain increment and stress increment is linear, i.e.,  $\dot{\epsilon}_{ij}^p = H_{ijkl} \dot{\sigma}_{kl}$ , where  $H_{ijkl}$  does not depend on the stress increment. This is an assumption that has been tested experimentally (see Drucker 1950).

### 2.3.3. Relations for $J_2$ flow theory

In  $J_2$  flow theory, we assume that the plastic deformation behavior is a function of the second stress invariant only. Initial yield occurs when the von Mises criterion is satisfied:

$$F(J_2) = J_2 = \frac{1}{3} \sigma_y^o{}^2 = \tau_y^o{}^2, \quad (2.73)$$

where  $\sigma_y^o$  and  $\tau_y^o$  are the yield stress in uniaxial tension and pure shear, respectively. Subsequent yield is governed by the following equation:

$$J_2 = J_2^{\max}. \quad (2.74)$$

In this equation  $J_2^{\max}$  is the maximum value of  $J_2$  over the entire prior stress history.  $J_2$  flow theory implies *isotropic strain hardening* (See Fig. 2.16). From tensile data alone, it is clear that this characterization is inadequate for reversed loading histories, since it ignores entirely the Bauschinger effect. For large amounts of reversed straining, however,  $J_2$  flow theory may give an accurate enough description.

Let's now formulate the relations for  $J_2$  flow theory. The normal to the yield surface is given by

$$\mu_{ij} = \frac{\partial F}{\partial \sigma_{ij}} = s_{ij}. \quad (2.75)$$

What are the conditions for loading and unloading? Well, when we are loading, we're pushing out the yield surface, so that

$$\text{Loading:} \quad J_2 = C \quad \text{and} \quad \dot{J}_2 = \mu_{ij} \dot{\sigma}_{ij} > 0.$$

We find similar conditions for neutral loading and unloading:

$$\text{Neutral loading: } J_2 = C \text{ and } \dot{J}_2 = \mu_{ij} \dot{\sigma}_{ij} = 0,$$

$$\text{Unloading: } J_2 = C \text{ and } \dot{J}_2 = \mu_{ij} \dot{\sigma}_{ij} < 0.$$

According to Drucker's postulates, the plastic strain increment must be perpendicular to the yield surface, i.e., it must scale with  $\mu_{ij} = s_{ij}$ . This condition is satisfied if the plastic strain increment is given by

$$\dot{\epsilon}_{ij}^p = \begin{cases} \frac{1}{h(J_2)} s_{ij} \dot{J}_2 & \text{for } \dot{J}_2 \geq 0 \text{ and } J_2 = J_2^{\max} \\ 0 & \text{for } \dot{J}_2 \leq 0, \end{cases} \quad (2.76)$$

where  $h$  is a function of just  $J_2$ . Why include  $\dot{J}_2$  in this expression? Well including it, ensures that we satisfy the Drucker inequality:

$$\dot{\epsilon}_{ij}^p \dot{\sigma}_{ij} = \frac{1}{h(J_2)} \dot{J}_2 s_{ij} \dot{\sigma}_{ij} = \frac{1}{h(J_2)} (\dot{J}_2)^2 > 0, \quad (2.77)$$

as long as  $h > 0$ . Taking into account Hooke's law for isotropic material, we find the total strain increments

$$\dot{\epsilon}_{ij} = \frac{1+\nu}{E} \dot{\sigma}_{ij} - \frac{\nu}{E} \dot{\sigma}_{pp} \delta_{ij} + \alpha h^{-1} s_{ij} \dot{J}_2, \quad (2.78)$$

where  $\alpha$  satisfies the following conditions:

$$\begin{aligned} \alpha &= 1 \quad \dot{J}_2 \geq 0, \\ \alpha &= 0 \quad \dot{J}_2 \leq 0. \end{aligned} \quad (2.79)$$

Equation (2.78) can be inverted to yield the stress increments as a function of strain increments

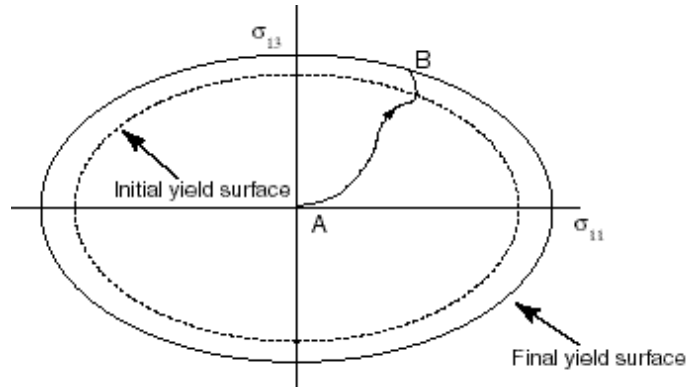


Fig. 2.16. Subsequent yield surface in  $J_2$  flow theory.



$$\dot{\sigma}_{ij} = \frac{E}{1+\nu} \left\{ \dot{\epsilon}_{ij} + \frac{\nu}{1-2\nu} \dot{\epsilon}_{pp} \delta_{ij} - \frac{\alpha s_{ij} s_{kl} \dot{\epsilon}_{kl}}{\frac{1+\nu}{E} h + 2J_2} \right\} \quad (2.80)$$

where

$$\begin{aligned} \alpha &= 1 \quad s_{mn} \dot{\epsilon}_{mn} \geq 0, \\ \alpha &= 0 \quad s_{mn} \dot{\epsilon}_{mn} \leq 0. \end{aligned} \quad (2.81)$$

The factor  $h(J_2)$  can be determined from any monotonic proportional loading history. Using *simple tension*, for example, we find that

$$J_2 = \frac{1}{3} \sigma^2, \quad s_{11} = \frac{2}{3} \sigma, \quad \dot{J}_2 = \frac{2}{3} \sigma \dot{\sigma}, \quad (2.82)$$

so that

$$\dot{\epsilon}^p = \frac{4}{9} \frac{1}{h(J_2)} \sigma^2 \dot{\sigma}. \quad (2.83)$$

From the experimental stress-strain curve we can determine the plastic strain

$$\dot{\epsilon}^p = \dot{\epsilon} - \dot{\epsilon}^e = \left( \frac{1}{E_t(\sigma)} - \frac{1}{E} \right) \dot{\sigma}. \quad (2.84)$$

Comparing both equations, then yields

$$h^{-1}(J_2) = \frac{9}{4} \frac{1}{\sigma^2} \left[ \frac{1}{E_t(\sigma)} - \frac{1}{E} \right] = \frac{3}{4J_2} \left[ \frac{1}{E_t(J_2)} - \frac{1}{E} \right], \quad (2.85)$$

which can be substituted into Eq. (2.78). It is often convenient to use the concept of equivalent stress  $\sigma_e$ :

$$\sigma_e = \sqrt{3J_2} = \sqrt{\frac{3}{2} s_{ij} s_{ij}}. \quad (2.86)$$

Note that in simple tension  $\sigma_e = \sigma$ . Thus, Eq. (2.85) can be written more explicitly in terms of equivalent stress:

$$h^{-1}(J_2) = \frac{9}{4} \frac{1}{\sigma_e^2} \left[ \frac{1}{E_t(\sigma_e)} - \frac{1}{E} \right]. \quad (2.87)$$

### 3. An example: Combined torsion and tension of a thin-walled tube

As an example that illustrates the properties of the plasticity equations introduced so far, we now consider the symmetric deformation of a circular thin-walled tube under the action of a twisting moment and an axial tension. We assume that the material is isotropic and that it is incompressible, i.e., Poisson's ratio is one half. The stress components different from zero are  $\sigma_{11}$  and  $\sigma_{13}$ , where the  $x_1$ -axis is taken parallel to the center axis of the tube, and the  $x_3$ -axis parallel to the hoop direction. The other stress components can be neglected. The strain components  $\varepsilon_{12}$  and  $\varepsilon_{23}$  can be neglected in comparison to  $\varepsilon_{13}$ . The von Mises yield criterion can be written in the  $(\sigma_{11}, \sigma_{13})$  plane as follows

$$\left(\frac{\sigma_{11}}{\sigma_y}\right)^2 + \left(\frac{\sigma_{13}}{\tau_y}\right)^2 = 1, \quad (2.99)$$

where  $\sigma_y$  and  $\tau_y$  are the yield stresses in uniaxial tension and shear, respectively. We introduce the following dimensionless variables:

$$\begin{aligned} q &= \frac{\sigma_{11}}{\sigma_y} & \tau &= \frac{\sigma_{13}}{\tau_y} \\ \eta &= \frac{\varepsilon_{11}}{\varepsilon_y} & \gamma &= \frac{\varepsilon_{13}}{\gamma_y} \end{aligned} \quad (2.100)$$

where  $\sigma_y = E\varepsilon_y$  and  $\tau_y = 2G\gamma_y$ . Introducing the dimensionless variables into the yield criterion leads to the following expression

$$\tau = \sqrt{1 - q^2}. \quad (2.101)$$

Let's now turn our attention to  $J_2$ -flow theory. We use the incremental relation

$$\dot{\varepsilon}_{ij} = \frac{1+\nu}{E} \dot{\sigma}_{ij} - \frac{\nu}{E} \dot{\sigma}_{pp} \delta_{ij} + \alpha h^{-1} s_{ij} \dot{J}_2, \quad (2.102)$$

to show that

$$\begin{aligned} \dot{\varepsilon}_{11} &= \frac{1}{E} \dot{\sigma}_{11} + \alpha h^{-1} \dot{J}_2 \frac{2}{3} \sigma_{11}, \\ \dot{\varepsilon}_{13} &= \frac{1+\nu}{E} \dot{\sigma}_{13} + \alpha h^{-1} \dot{J}_2 \sigma_{13} = \frac{3}{2E} \dot{\sigma}_{13} + \alpha h^{-1} \dot{J}_2 \sigma_{13}. \end{aligned} \quad (2.103)$$

After introducing the dimensionless variables, we find

$$\dot{\eta} = \dot{q} + \alpha h^{-1} J_2 \frac{2}{3} E q, \quad (2.104)$$

$$\dot{\gamma} = \dot{\tau} + \alpha h^{-1} J_2 \frac{2}{3} E \tau.$$

After eliminating  $\alpha h^{-1} J_2$  from these equations, we find

$$\frac{\dot{\eta} - \dot{q}}{\dot{\gamma} - \dot{\tau}} = \frac{q}{\tau}. \quad (2.105)$$

Eliminating  $\tau$  from Eqs. (2.104) and (2.105), leads to the following non-linear differential equation in  $q$ :

$$\frac{\dot{q}}{\dot{\eta}} = 1 - q^2 - q \sqrt{1 - q^2} \frac{\dot{\gamma}}{\dot{\eta}}. \quad (2.106)$$

It must be emphasized that in order to determine  $q$  from this equation, it is necessary to prescribe the deformation path  $\gamma = \gamma(\eta)$ . Some solutions for various strain paths are shown in Fig. 2.17.

**Exercises:**

Calculate  $q$  for the following two deformation paths;

- A linear deformation path  $\gamma(\eta) = A + B\eta$
- A step-like deformation path consisting respectively of two segments  $\eta = \text{constant}$  and  $\gamma = \text{constant}$ .

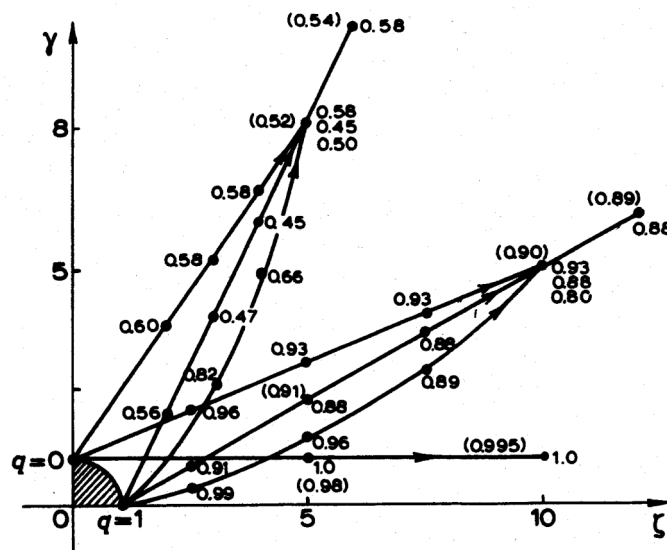


Fig. 2.17. Solutions for a thin-walled circular tube for various stress histories.

#### 4. Application: The thick-walled hollow sphere (Adapted from Lubliner)

Like the problem of a tube under torsion, that of an axisymmetrically loaded shell of revolution is statically determinate when the shell is thin walled, but ceases to be so when the shell is thick-walled.

##### 4.1. Elastic Hollow Sphere under Internal and External Pressure

###### Basic Equations

In a hollow sphere of inner radius  $a$  and outer radius  $b$ , subject to normal pressures on its inner and outer surfaces, and made of an isotropic materials, the displacement and stress fields must be spherically symmetric. The only non-vanishing displacement component is the radial displacement,  $u$ , a function of the radial coordinate  $r$  only. The only non-vanishing strains are the radial and circumferential strains:

$$\varepsilon_r = \frac{du}{dr} \text{ and } \varepsilon_\theta = \varepsilon_\varphi = \frac{u}{r}.$$

The strains obviously satisfy the compatibility condition

$$\varepsilon_r = \frac{d}{dr}(r\varepsilon_\theta). \quad (4.3.1)$$

The only non-vanishing stress components are the radial stress  $\sigma_r$  and the circumferential stresses  $\sigma_\theta = \sigma_\varphi$ , which satisfy the equilibrium equation

$$\frac{d\sigma_r}{dr} + 2\frac{\sigma_r - \sigma_\theta}{r} = 0. \quad (4.3.2.)$$

###### Elastic solution

The strain-stress relations for an isotropic linearly elastic solid reduce in the present case to

$$\begin{aligned} \varepsilon_r &= \frac{1}{E}(\sigma_r - 2\nu\sigma_\theta), \\ \varepsilon_\theta &= \frac{1}{E}[(1-\nu)\sigma_\theta - \nu\sigma_r] \end{aligned}$$

The compatibility equation Eq.(4.3.1) may now be rewritten in terms of the stresses to read

$$\frac{d}{dr}[(1-\nu)\sigma_\theta - \nu\sigma_r] + \frac{1+\nu}{r}(\sigma_\theta - \sigma_r) = 0,$$

which with the help of Eq. (4.3.2) reduces to

$$\frac{d}{dr}(\sigma_r + 2\sigma_\theta) = 0.$$

The quantity  $\sigma_r + 2\sigma_\theta$  is accordingly equal to a constant, say  $3A$ . Furthermore, we find that

$$\frac{d\sigma_\theta}{dr} = -\frac{1}{2} \frac{d\sigma_r}{dr},$$

so that

$$\frac{2}{3} \frac{d(\sigma_\theta - \sigma_r)}{dr} = -\frac{d\sigma_r}{dr}.$$

Equation (4.3.2) may then be rewritten as

$$\frac{d}{dr}(\sigma_\theta - \sigma_r) + \frac{3}{r}(\sigma_\theta - \sigma_r) = 0,$$

leading to the solution

$$\sigma_\theta - \sigma_r = \frac{3B}{r^3},$$

where  $B$  is another constant. The stress field is therefore given by

$$\sigma_r = A - \frac{2B}{r^3}, \quad \sigma_\theta = A + \frac{B}{r^3}.$$

With the boundary conditions

$$\sigma_r|_{r=a} = -p_i, \quad \sigma_r|_{r=b} = -p_e,$$

where  $p_i$  and  $p_e$  are the interior and exterior pressures, respectively, the constant  $A$  and  $B$  can be solved for, and the stress components  $\sigma_r$  and  $\sigma_\theta$  can be expressed as

$$\sigma_r = -\frac{1}{2}(p_i + p_e) + \frac{p_i - p_e}{2[1 - (a/b)^3]} \left[ 1 + \left(\frac{a}{b}\right)^3 - 2\left(\frac{a}{r}\right)^3 \right],$$

$$\sigma_\theta = -\frac{1}{2}(p_i + p_e) + \frac{p_i - p_e}{2[1 - (a/b)^3]} \left[ 1 + \left(\frac{a}{b}\right)^3 + \left(\frac{a}{r}\right)^3 \right],$$

that is, the stress field is the superposition of a uniform stress field equal to the negative of the average of the external and internal pressures and a variable stress field proportional to the pressure difference.

#### *Sphere Under Internal Pressure Only*

The preceding solution is due to Lamé. It becomes somewhat simpler if the spheres is subject to an internal pressure only with  $p_i = p$  and  $p_e = 0$ . The stresses are then

$$\sigma_r = -\frac{p}{(b/a)^3 - 1} \left( \frac{b^3}{r^3} - 1 \right),$$

$$\sigma_\theta = \frac{p}{(b/a)^3 - 1} \left( \frac{b^3}{2r^3} + 1 \right),$$

If the sphere material is elastic-plastic, then the largest pressure for which the preceding solution is valid is that at which the stresses at some  $r$  first satisfy the yield criterion; this limiting pressure will be denoted  $p_E$ . Since two of the principal stresses are equal, the stress state is equibiaxial, and both the Tresca and Von Mises yield criteria reduce to

$$\sigma_\theta - \sigma_r = \sigma_Y \quad (4.3.3)$$

where  $\sigma_Y$  is the tensile yield stress, since  $\sigma_\theta > \sigma_r$  everywhere. The value of  $\sigma_\theta - \sigma_r$  is maximum at  $r = a$ , where it attains  $3p/2[1 - (a/b)^3]$ . The largest pressure at which the sphere is wholly elastic is therefore

$$p_E = \frac{2}{3} \sigma_Y \left( 1 - \frac{a^3}{b^3} \right). \quad (4.3.4)$$

#### **4.2. Elastic-Plastic Hollow Sphere Under Internal Pressure**

##### *Stress Field*

When the pressure in the hollow sphere exceeds  $p_E$ , a spherical domain of inner radius  $a$  and outer radius  $c$  becomes plastic. The elastic domain  $c < r < b$  behaves like an elastic shell of inner radius  $c$  that is just yielding at  $r = c$ , so that  $\sigma_r$  and  $\sigma_\theta$  are given by

$$\sigma_r = -\frac{p_c}{(b/c)^3 - 1} \left( \frac{b^3}{r^3} - 1 \right),$$

$$\sigma_\theta = \frac{p_c}{(b/c)^3 - 1} \left( \frac{b^3}{2r^3} + 1 \right),$$

where  $p_c = -\sigma_r(c)$  is such that the yield criterion is met at  $r = c$ , that is, it is given by the right-hand side of Eq. (4.3.4) with  $a$  replaced by  $c$ :

$$p_c = \frac{2}{3} \sigma_Y \left( 1 - \frac{c^3}{b^3} \right)$$

Therefore,

$$\sigma_r = -\frac{2}{3} \sigma_Y \left( \frac{c^3}{r^3} - \frac{c^3}{b^3} \right),$$

$$\sigma_{\theta} = \frac{2}{3}\sigma_y \left( \frac{c^3}{2r^3} + \frac{c^3}{b^3} \right) \quad c < r < b. \quad (4.3.5)$$

In particular,  $\sigma_{\theta}(b) = \sigma_y (c/b)^3$ .

In the plastic domain, the yield criterion Eq. (4.3.3) holds everywhere, so that the equilibrium equation Eq. (4.3.2) may be integrated for  $\sigma_r$ , subject to continuity with the elastic solution at  $r = c$ , to yield,

$$\sigma_r = -\frac{2}{3}\sigma_y \left( 1 - \frac{c^3}{b^3} + \ln \frac{c^3}{r^3} \right),$$

assuming the solid is ideally plastic. We immediately obtain  $\sigma_{\theta} = \sigma_r + \sigma_y$

$$\sigma_{\theta} = \frac{1}{3}\sigma_y \left( 1 + 2\frac{c^3}{b^3} - 2\ln \frac{c^3}{r^3} \right).$$

The radius  $c$  marking the extent of the plastic domain is obtained, at a given pressure  $p$ , from the condition that  $\sigma_r(a) = -p$ , or

$$p = \frac{2}{3}\sigma_y \left( 1 - \frac{c^3}{b^3} + \ln \frac{c^3}{a^3} \right). \quad (4.3.6)$$

When  $c = b$ , the shell is completely plastic. The corresponding pressure is the *ultimate pressure*, given by

$$p_U = 2\sigma_y \ln \frac{b}{a}.$$